Regional feedbacks among fire, climate, and tropical deforestation

William A. Hoffmann[1]

Departamento de Engenharia Florestal, Universidade de Brasília, Brasília, Brazil

Wilfrid Schroeder

Instituto Brasileiro do Meio Ambiente e dos Recursos Naturais Renováveis, Brasília, Brazil

Robert B. Jackson

Department of Biology and Nicholas School of the Environment and Earth Sciences, Duke University, Durham, North Carolina, USA

[1] Numerous studies with general circulation models suggest that tropical deforestation can result in regional-scale climate change; namely, increased air temperature and wind speed and reduced precipitation and relative humidity. To quantify how this climate change should affect fire risk, we used the National Center for Atmospheric Research (NCAR) CCM3.2 general circulation model and remote sensing to estimate the effect of tropical deforestation on fire risk through the McArthur forest fire danger index (FFDI). Deforestation reduced precipitation and relative humidity and increased wind speed in the Amazon, Congo, and Indonesia/New Guinea. FFDI increased by 41, 56, and 58% in these three regions, respectively, primarily owing to higher wind speeds and reduced precipitation. Actual fire occurrence in the Amazon, as determined from NOAA-12 images, was strongly correlated with the FFDI calculated from meteorological data ($P \ll 0.0001$). Using the observed relationship between FFDI and fire occurrence, we estimate increases in fire frequency of 44, 80, and 123%, in the Amazon, Congo, and Indonesia, respectively, with deforestation. In all three regions the largest relative increases in fire risk occurred in the more humid areas with the lowest original fire risk. *INDEX TERMS:* 0315 Atmospheric Composition and Structure: Biosphere/atmosphere interactions; 3360 Meteorology and Atmospheric Dynamics: Remote sensing; 3210 Mathematical Geophysics: Modeling; 3322 Meteorology and Atmospheric Dynamics: Land/atmosphere interactions; *KEYWORDS:* tropical forest, fire, GCM modeling, remote sensing, fire meteorology, climate change

1. Introduction

[2] Uncontrolled fire is a principal factor contributing to the degradation of deforested and selectively logged tropical forests. Thinning or removal of the forest canopy permits greater insolation at the soil surface, which dries fuel, increases air temperature and reduces relative humidity near the soil [*Uhl and Kauffman*, 1990]. So although undisturbed tropical forest is not typically flammable, even during moderate drought, selectively logged forest and areas cleared for pasture are prone to burning [*Holdsworth and Uhl*, 1997; *Uhl and Kauffman*, 1990]. Large areas of pasture and selectively logged forest burn annually [*Cochrane et al.*, 1999; *Nepstad et al.*, 1999]. This burning further reduces tree cover and prevents tree regeneration, resulting in a positive feedback at the local scale [*Cochrane et al.*, 1999; *Cochrane and Schulze*, 1999; *Nepstad et al.*, 2001].

[3] In addition to local changes in microclimate, regional climate change resulting from large-scale deforestation should contribute further to this vegetation-climate feedback [*Laurance and Williamson*, 2001; *Hoffmann and Jackson*, 2000; *Hoffmann et al.*, 2002; *Nepstad et al.*, 2001]. Simulations with general circulation models (GCMs) have repeatedly demonstrated that changes in albedo, roughness length, leaf-area index and rooting depth caused by tropical deforestation reduce precipitation and relative humidity and increase surface temperature and wind speed [*Dickinson and Kennedy*, 1992; *Hahmann and Dickinson*, 1997; *Henderson-Sellers et al.*, 1993; *Nobre et al.*, 1991; *Polcher and Laval*, 1994; *Sud et al.*, 1996; *Zeng et al.*, 1996; *Zhang et al.*, 1996]. All four of these climatic changes should increase fire risk [*Hoffmann et al.*, 2002; *Noble et al.*, 1980].

[4] Although these changes are often described as regional effects of deforestation, such GCM results combine both local and regional effects [*Salati and Nobre*, 1991]. Distinguishing between regional and local climate change is

---

[1]Now at Department of Botany, North Carolina State University, Raleigh, North Carolina, USA.

Table 1. Relevant Surface Characteristics Used in the Simulations[a]

Parameter	Forest	Pasture
Albedo	10.130	0.176
Root distribution parameter	0.972[b]	0.943[b]
Roughness length	2.62	0.06
Jan. LAI	4.5	1.8
Feb. LAI	4.5	1.4
Mar. LAI	4.5	1.1
Apr. LAI	4.5	1.7
May LAI	4.5	2.2
June LAI	4.5	2.8
July LAI	4.5	3.3
Aug. LAI	4.5	3.3
Sep. LAI	4.5	3.3
Oct. LAI	4.5	3.3
Nov. LAI	4.5	2.7
Dec. LAI	4.5	2.1
Jan. SAI	0.5	0.3
Feb. SAI	0.5	0.3
Mar. SAI	0.5	0.3
Apr. SAI	0.5	0.4
May SAI	0.5	0.5
June SAI	0.5	0.5
July SAI	0.5	0.6
Aug. SAI	0.5	0.6
Sep. SAI	0.5	0.6
Oct. SAI	0.5	0.6
Nov. SAI	0.5	0.5
Dec. SAI	0.5	0.5
Leaf VIS reflectance	0.095	0.1056
Leaf NIR reflectance	0.428	0.5568
Leaf VIS transmittance	0.0475	0.0475
Leaf NIR transmittance	0.2375	0.2112
Stem VIS reflectance	0.152	0.3456
Stem NIR reflectance	0.37	0.5568
Stem VIS transmittance	0.00095	0.2112
Stem NIR transmittance	0.00095	0.3648

[a]Note that albedo is not prescribed directly in LSM, but is calculated from the leaf area index (LAI), stem area index (SAI), as well as the reflectances and transmittances of the leaves and stems. LAI and SAI values are for the Northern Hemisphere; for the Southern Hemisphere, the values are offset by 6 months.

[b]For these root distribution parameters, 99% of root surface area occurs in the top 162 cm of soil for forest trees and in the top 78 cm for pasture grass.

important because the two are likely to have very different impacts on fire occurrence. If the changes are entirely local, the increased fire risk would be limited only to disturbed sites and would be relatively unaffected by the regional extent of deforestation. In contrast, a regional component to this feedback could extend the increased fire risk to undisturbed areas and would depend more strongly on the scale of deforestation.

[5] Here we focus on the regional effects of tropical deforestation on fire occurrence, using GCM simulations and remote sensing to answer the following questions: What are the predicted changes in fire risk and fire occurrence due to tropical deforestation? What are the relative contributions of precipitation, relative humidity, wind speed, and temperature to this overall change in fire risk? How does the increase in fire risk respond to the scale of deforestation?

2. Model and Simulations

[6] Simulations were run using the NCAR Community Climate Model (CCM3.2) with a spatial resolution of approximately $2.8° \times 2.8°$ of Earth's surface (T42 spectral truncation) and 18 vertical levels. A detailed model description is available from *Kiehl et al.* [1998]. CCM3.2 is coupled with the NCAR Land Surface Model (LSM) described by *Bonan* [1996]. LSM simulates the fluxes of momentum, radiation, latent heat and sensible heat between the land and the atmosphere. An analysis of the control climatology of CCM3.2/LSM is presented by *Bonan* [1998].

[7] Within LSM, each grid cell of the vegetated surface of Earth is assigned one of 28 vegetation types. Each vegetation type is composed of one or more plant types and/or bare soil. When vegetation is composed of more than one plant type, surface variables as well as fluxes of water, energy, and momentum are averaged over separate vegetation subgrid cells, each occupied by the respective plant type. A total of 12 plant types are represented in LSM, differing in leaf area, stem area, root profile, leaf dimension, optical properties, stomatal physiology, roughness length, and displacement height. We added a new plant type 'pasture grass' for use in the deforestation scenarios. The LAI of pasture grass was changed to correspond to data from the Anglo-Brazilian Amazonian Climate Observation Study (ABRACOS) project made available by the UK Institute of Hydrology and the Instituto Nacional de Pesquisas Espaciais (Brazil).

[8] In LSM, albedo is not prescribed as a single parameter, but is calculated with a two-stream radiation procedure based on LAI, leaf optical properties, and leaf orientation. Leaf optical properties of broadleaf evergreen trees and pasture grass were adjusted to ensure that simulated albedos corresponded to values measured over forest and pasture in the Amazon by ABRACOS (Table 1). This was done by performing offline simulations of the two-stream procedure of LSM and adjusting the leaf and stem transmittances and reflectances accordingly. Following this adjustment, initial one-year simulations were performed for both the control and deforested scenarios, yielding average albedo values of 13.0% and 17.6%, close to measured values of 13.2% and 17.6% (ABRACOS). Finally, the empirical rooting parameter β was obtained from the database of *Jackson et al.* [1997]. This unitless parameter is defined by the relation $Y = 1 - \beta^d$, where Y is the cumulative root fraction from the soil surface to depth d (cm) [*Jackson et al.*, 2000].

[9] The use of subgrid cells of different cover types makes LSM useful for examining local versus regional effects of deforestation. In LSM, surface variables and fluxes are normally simulated for each subgrid cover type and a weighted average is calculated over all subgrid cells of a given grid cell. For model output, we changed this spatial averaging, analyzing these variables only over pasture grass subgrid patches, while retaining the usual subgrid averaging for feeding the atmospheric model. To permit this, a small area of pasture grass (5%) was included in control (forest) simulation. So in all scenarios, wind speed, surface air temperature, and relative humidity (RH) were analyzed only over pasture grass cover types, ensuring that any change in these variables is due to regional changes rather than local changes caused by the underlying vegetation.

[10] In all simulations performed here, the daily values of precipitation, maximum wind speed at 10m height, maximum air temperature, and minimum RH were used to calculate the McArthur Forest Fire Danger Index [*Noble et al.*, 1980]. This index was developed to provide a
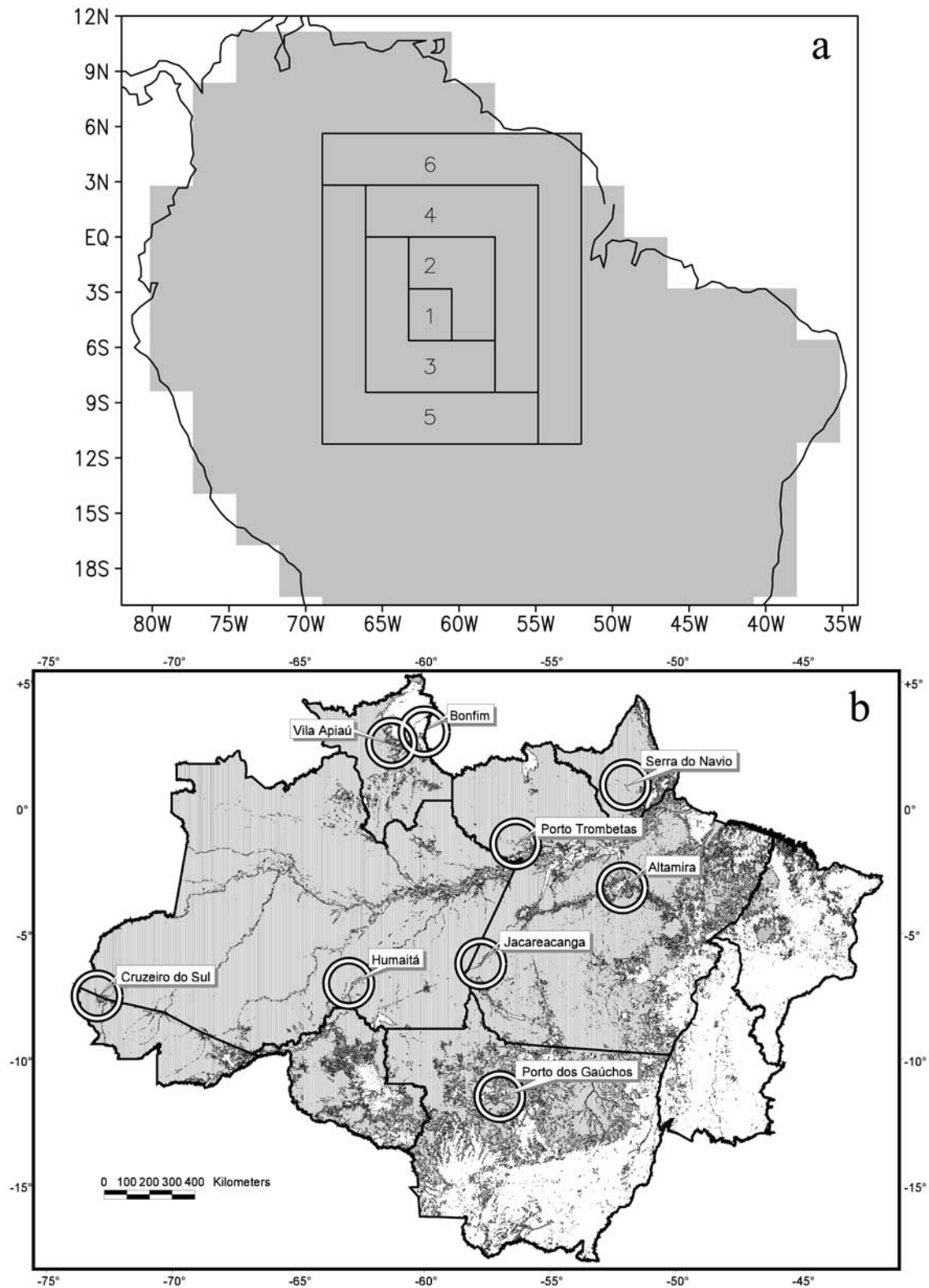
Figure 1. (a) Area subjected to deforestation in experiment 2. In the second experiment, six scenarios were simulated, with 1, 4, 9, 16, 25, and 36 grid cells deforested, respectively. The numbered regions 1 to 6 indicate the sequence of progressive increase in deforested area, i.e., in the one-cell scenario, area 1 was deforested; in the four-cell scenario, areas 1 and 2 were deforested, etc. (b) The nine areas within which daily counts of NOAA-12 hot spots were obtained within the Brazilian Amazon. Each is an area defined by a 100km radius around a meteorological station. Shading indicates forest and white indicates deforested and savanna ecosystems.

Table 2. Simulated Effects of Vegetation Change on Mean Annual Values of the Four Meteorological Variables Used to Calculate the Forest Fire Danger Index (FFDI)

	Precipitation, mm yr^{-1}		Maximum Temperature, °C		Maximum Wind Speed, m s^{-1}		Minimum Relative Humidity, %		Forest Fire Danger Index	
	Control	Change	Control	Change	Control	Change	Control	Change	Control	Change
Amazon	2024	−683[a]	32.4	−0.3[a]	3.6	+1.9[a]	60.6	−4.9[a]	7.00	+2.90[a]
Africa	2530	−648[a]	30.8	−0.3[a]	3.4	+1.6[a]	64.8	−4.7[a]	4.33	+2.44[a]
SE Asia	1023	−86[b]	28.0	−1.3[a]	4.2	+1.5[a]	54.5	+3.2[a]	8.57	−0.99[b]
Indonesia	2524	−431[a]	29.4	−0.0[c]	2.9	+1.3[a]	77.1	−1.9[a]	1.36	+0.79[a]
Average	2039	−549	31.2	−0.4	3.6	+1.7	62.8	−3.2	5.93	+1.92

[a]$P < 0.005$.
[b]$P < 0.01$.
[c]Not significant.

quantitative measure of fire risk directly related to the probability of fire occurrence and to the rate of spread. It is calculated as

$$FFDI = 2.0 \exp(-0.450 - 0.0345H + 0.0338T + 0.0842V + 0.987 \ln(D)), \quad (1)$$

where H is minimum RH (%), T is maximum air temperature (°C), V is maximum wind velocity at 10 m in the open (m/s), and D is a drought factor [*Noble et al.*, 1980]. The drought factor, which is restricted to values less than 10, is

$$D = \frac{0.191*(I + 104)(N + 1)^{1.5}}{3.52(N + 1)^{1.5} + P - 1}, \quad (2)$$

where N is the number of days without rain, and P is the amount of precipitation (mm) of the last rainfall event [*Noble et al.*, 1980]. The Keech-Byram drought index (I), is calculated based on the time series of past precipitation events and maximum daily temperatures [*Keetch and Byram*, 1968].

[11] Surface RH was calculated at the LSM reference height (2 m above zero plane displacement). Wind speed at 10 m was calculated as

$$u_{10} = u_*(\ln((10 - d)/z_o) - \psi_m)/k, \quad (3)$$

where u_* is friction velocity, d is zero-plane displacement, z_0 is roughness length, k is the von Karman constant, and Ψ_m is the stability correction factor [*Garratt*, 1992].

2.1. Experiment 1

[12] Climate was simulated under three scenarios: control (forest), partial deforestation, and complete deforestation (pasture). In the control scenario, the vegetation was composed of 95% broadleaf evergreen tree and 5% pasture grass. In the complete deforestation scenario it was composed of 90% pasture grass and 10% bare soil. The partial deforestation scenario was intermediate, with 47.5% broadleaf evergreen tree, 47.5% pasture grass, and 5% bare soil.

[13] The forest and deforested simulations were run for 13 model years, while the partial deforestation simulation was run for 9 years. In all cases, the first year of simulation was discarded as a spin-up to the actual simulation. Simulations were run with AMIP sea surface temperatures.
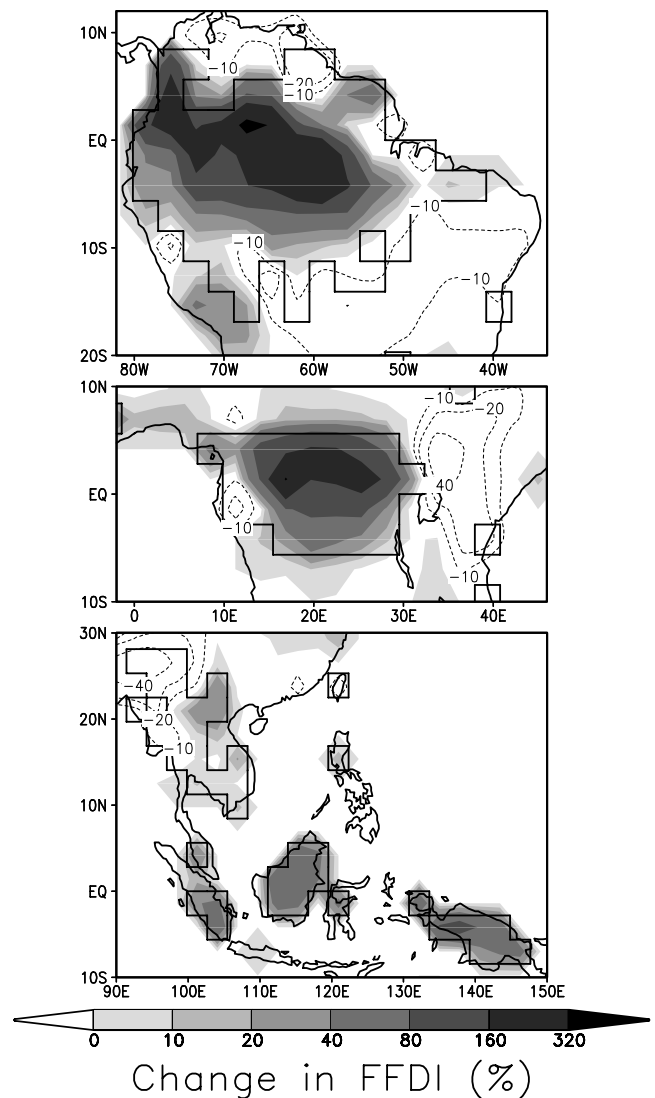
Figure 2. The effect of deforestation on the McArthur Forest Fire Danger Index (FFDI) in (top) the Amazon basin, (middle) the Congo Basin, and (bottom) southeast Asia, Indonesia, and New Guinea. The outlined areas were the tropical forest regions subjected to the deforestation scenario. See color version of this figure in the HTML.
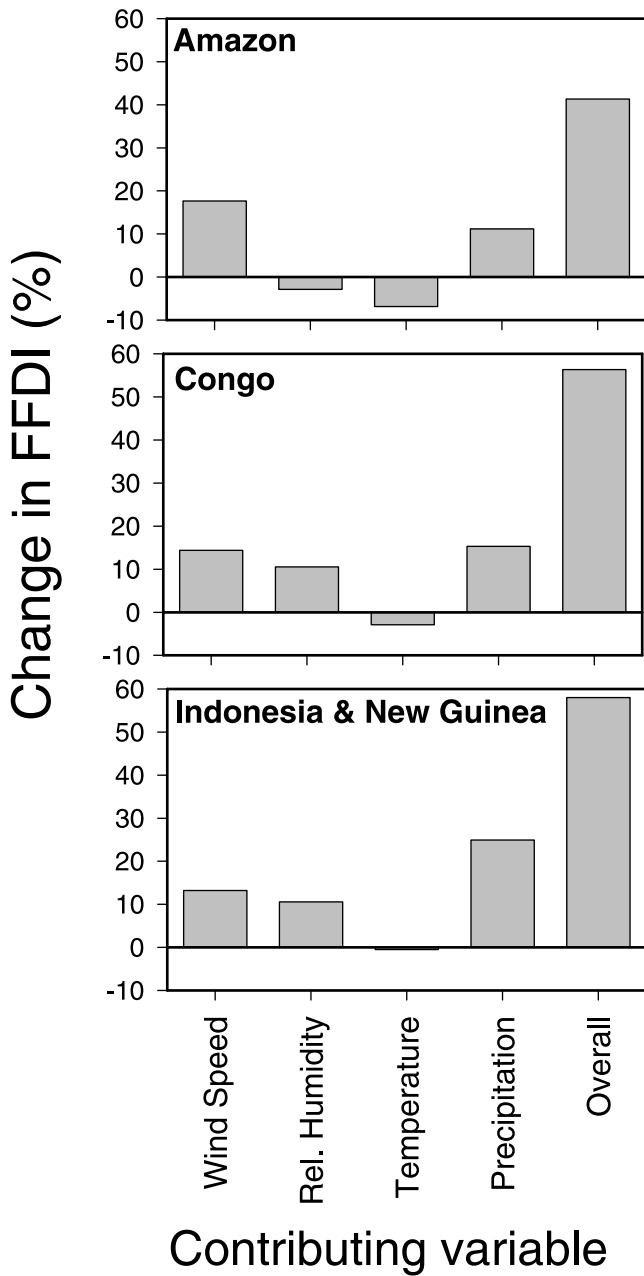
Figure 3. Contribution of the various meteorological variables to the overall increase in the forest fire danger index (FFDI).

precipitation, and temperature taken from the control scenario, along with wind speed taken from the deforested scenario. This estimates the change in FFDI resulting from a change in only one variable at a time.

[16] To relate fire risk to the El Niño Southern Oscillation (ENSO), we used the Southern Oscillation Index (SOI)

[14] The t-test was used to compare scenarios. Daily output was first averaged over all grid cells in a region (Amazon, Congo, SE Asia, Indonesia), and the t-test performed on these daily means. To correct for temporal autocorrelation in these daily values, the degrees of freedom were adjusted as recommended by *Zwiers and von Storch* [1995].

[15] We calculated the contribution of each of the four meteorological variables to the overall increase in FFDI. This was done by calculating FFDI using output from the forest scenario, but substituting the values of one of the four variables from the deforested scenarios. For example, to determine the contribution of increased wind speed to the overall increase in fire risk, FFDI was calculated from RH,

Figure 4. Relationship between FFDI and number of remotely sensed hot spots observed within a 100 km radius. Each point represents the mean of ≥50 days of observations.
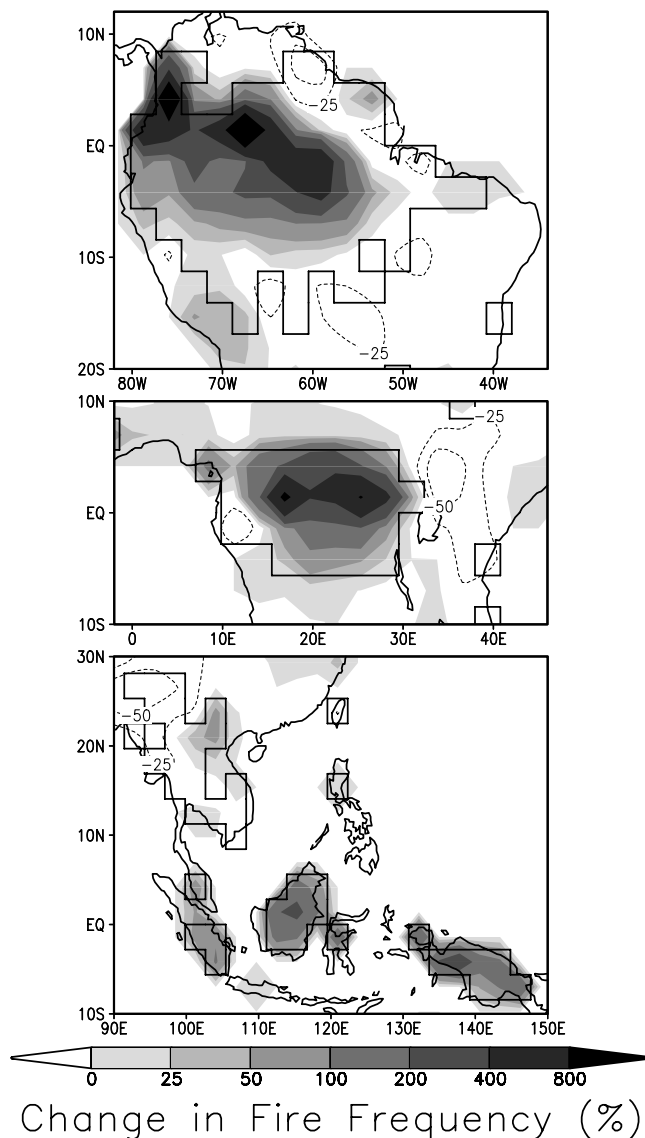
Figure 5. The predicted increase in fire occurrence due to the regional climate change provoked by complete deforestation. See color version of this figure in the HTML.

calculated as described by *Trenberth* [1984] and available from the NCAR Climate Analysis Section at http://www.cgd.ucar.edu/cas/catalog/climind/soi.html.

2.2. Experiment 2

[17] These simulations were performed to determine the effect of increasing area of deforestation on climate and fire risk. Six simulations were run using the same vegetation compositions as in experiment 1, but with deforested areas of 1, 4, 9, 16, 25, and 36 grid cells (2.8° square) in the Amazon region. The deforested areas of the six scenarios were nested within each other, as shown in Figure 1a. Each simulation was run for six years.

3. Meteorological Data and Remote Sensing

[18] To relate FFDI to actual fire activity, FFDI was calculated for 1998–2002 at nine sites in the Amazon basin

from meteorological data obtained from the Centro de Previsão do Tempo e Estudos Climáticos (CPTEC/INPE, Figure 1b). These were chosen from the 20 stations managed by CPTEC within Brazilian Legal Amazon, because they had the most complete data sets. We eliminated one station (São Gabriel da Cachoeira) because fires were detected on only four dates during the study period.

[19] Daily fire counts within a 100km radius of each meteorological station were obtained from the evening pass (16:30 to 17:30 local time) of NOAA-12. Evening passes were used to avoid spurious hot spots from warm or bright surfaces. To avoid any potential problems resulting from uncertainty in the absolute area or number of fires, we limit our interpretation to relative changes in fire number.

4. Results

[20] Deforestation had a substantial effect on the climate of the tropical forest regions examined. Precipitation declined by 34% in the Amazon basin, 26% in the Congo basin, 8% in Southeast Asia, and 17% over Indonesia and New Guinea (Table 2). Mean daily maximum wind speed increased by nearly half $(1.3 - 1.9 \text{ m s}^{-1})$ in all four regions (Table 2). Air temperature at reference height in the open declined slightly, but significantly in the Amazon, Congo, and SE Asia. Minimum RH declined by >4.5% in the Amazon and Congo basins and by 1.9% in Indonesia and New Guinea, while increasing in Southeast Asia (Table 2).

[21] As a result of these changes in climate, McArthur Forest Fire Danger Index increased by 41%, 56%, and 58% in the Amazon, the Congo, and Indonesia/New Guinea (Table 2, Figure 2). However, FFDI declined by 12% in Southeast Asia (Table 2). In the Amazon, the increase in FFDI in the deforested scenario was due entirely to reduced precipitation and increased wind speed, whereas in the Congo and Indonesia, reduced RH also contributed considerably (Figure 3).

[22] The observed number of hot spots was significantly correlated to FFDI at each of the nine study sites (Figure 4; F > 51.1, $P \ll 0.0001$), and for the pooled data (F = 740.4, $P \ll 0.0001$). Pooling data from all sites yielded the function H = 0.0879*FFDI$^{1.891}$, where H is the number of hot spots observed in a day. Using this relationship to estimate the increase in fire occurrence caused by deforestation, we predict fire occurrence to increase 43.9%, 79.5%, and 123% in the Amazon, Congo and Indonesia/New Guinea, respectively (Figure 5). In contrast, fire occurrence is predicted to decline by 24% in SE Asia. Within the Congo and Amazon regions, the increase was not uniform, with large areas showing more than a four-fold increase in predicted fire number. These areas of greatest increase lie within the humid equatorial regions with the lowest initial fire risk. In many areas peripheral to the deforested regions, there was a reduction in fire risk in the deforested scenario (Figures 2 and 5) relative to the control. This reduction was associated with increased precipitation and relative humidity and reduced surface air temperature (data not shown).

[23] These predictions of climate change are based on the unrealistic scenario of complete deforestation over entire regions. However, even partial deforestation should provoke a change in climate and fire risk as shown by the nearly linear responses of FFDI, predicted fire number, and the
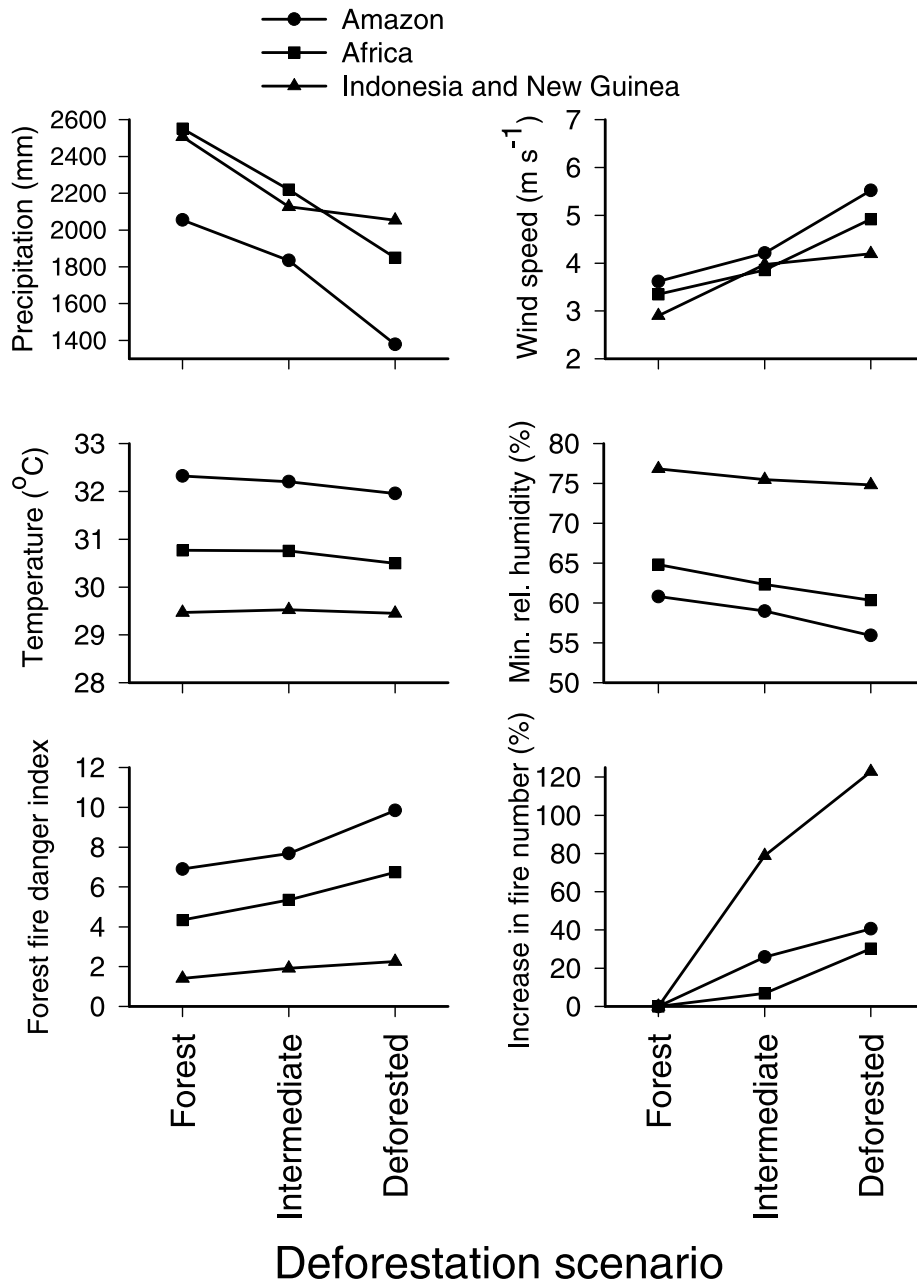
Figure 6. Relationship between completeness of deforestation and climate. In the intermediate scenario, forest cover in each grid cell was reduced by half, and in the deforested scenario, all forest cover was removed.

four meteorological variables to percent deforestation (Figure 6). Similarly, the magnitude of change in all of these variables depends on the total area deforested (Figure 7).

[24] Fire risk in the Amazon and in Indonesia was negatively, but weakly, correlated to the Southern Oscillation Index (Figure 8, $0.059 < r^2 < 0.162$, $P < 0.003$). Negative values of the SOI indicate El Niño conditions, so greatest fire risk was observed in El Niño years.

5. Discussion

[25] The simulated climate change caused by tropical deforestation substantially increased fire risk and predicted

fire number. This increased fire risk due to regional climate change is additional to that caused by local microclimatic changes in degraded and deforested sites. Both the local microclimatic change and the regional climate change are likely to contribute to a positive feedback loop in which deforestation results in increased fire frequency and further reductions in tree cover.

[26] The positive feedback provoked by the local effects of deforestation is already very evident in the Amazon. When a forest is degraded by selective logging, a more open canopy permits higher understory temperatures, lower relative humidity, and more rapid fuel drying. Consequently, the forest becomes much more flammable, permitting large
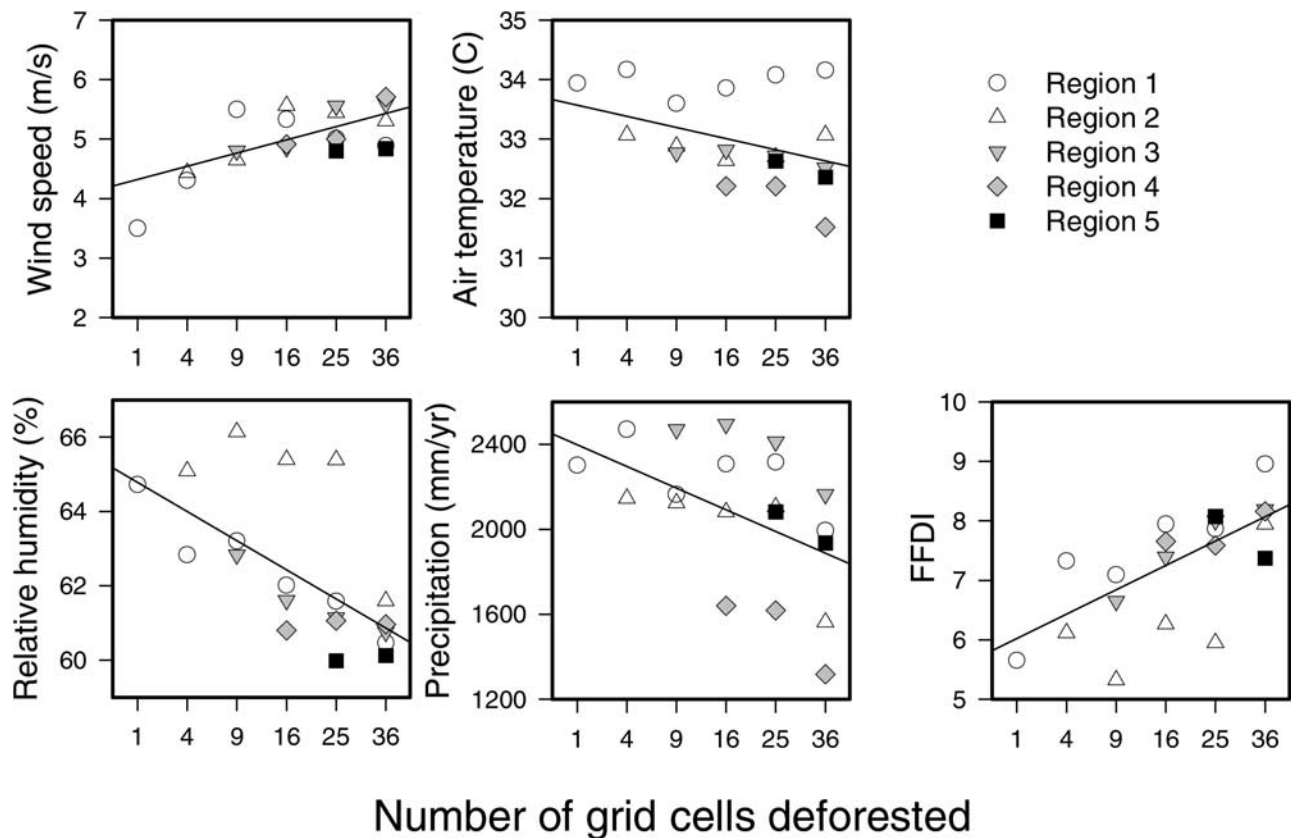
Figure 7. Relationship between deforested area and climate. The fitted lines represent the average slope through the points of the separate regions, as determined by analysis of covariance. The five regions refer to the nested blocks in Figure 1.

areas of degraded forests to burn every year [*Cochrane et al.*, 1999; *Nepstad et al.*, 1999], causing widespread tree mortality and impeding further regeneration. Thus, by preventing canopy closure, fire maintains conditions that promote future fires.

[27] Although these microclimatic effects of deforestation do not extend more than a few tens of meters into forest patches [*Davies-Colley et al.*, 2000; *Giambelluca et al.*, 2003; *Newmark*, 2001], the regional climate change examined in the present study should increase fire risk in areas not directly degraded by humans. In consequence, even large, well-protected forest reserves may be affected. Primary tropical forest typically requires prolonged drought to become flammable, so in most years relatively little undisturbed forest burns. However, due to regional climate change, these conditions will likely be met more frequently in the remaining forest patches.

[28] Unlike the local changes in microclimate, regional climate change depends on the spatial extent of deforestation. FFDI and the meteorological variables were all correlated with the number of grid cells deforested (Figure 7). Furthermore, FFDI was nearly linearly related to the fraction of deforestation within grid cells (Figure 6). These two results indicate that even partial deforestation could worsen the problem of fire in tropical forests.

[29] The increased fire risk in the deforestation scenario was caused by increased wind speed and reduced precipitation and relative humidity. Air temperature, which de-

creased in response to deforestation, did not contribute to the increased fire risk. This decline in temperature was unexpected, as other deforestation studies have almost invariably shown an increase in surface temperature. In the present study, however, air temperature, along with wind speed and relative humidity, was obtained exclusively over pasture subgrid cells in all scenarios to control for the local effects of underlying vegetation. When averaged over all subgrid cells in these simulations, as is typically done in LSM, deforestation causes an increase of $\sim 1.7°C$ (data not shown), a change comparable to other GCM studies. The increase in air temperature due to deforestation is caused principally by a reduction in roughness length [*Eltahir and Bras*, 1993; *Hahmann and Dickinson*, 1997; *Hoffmann and Jackson*, 2000], but this effect disappears when we control for underlying vegetation type, indicating that it is a local effect of deforestation limited to the sites where deforestation occurs. In reality, we would expect the increased air temperature to extend a few tens of meters into surrounding areas [*Davies-Colley et al.*, 2000; *Giambelluca et al.*, 2003; *Newmark*, 2001], but LSM does not allow for such advection among subgrid patches.

[30] Here, air temperature over pasture patches actually declined in response to deforestation of the remaining forest, probably due to the increased wind speed, which facilitates the dissipation of sensible heat to the atmosphere.

[31] Deforestation caused the greatest relative increases in fire risk in the humid equatorial zone (Figures 2 and 5).
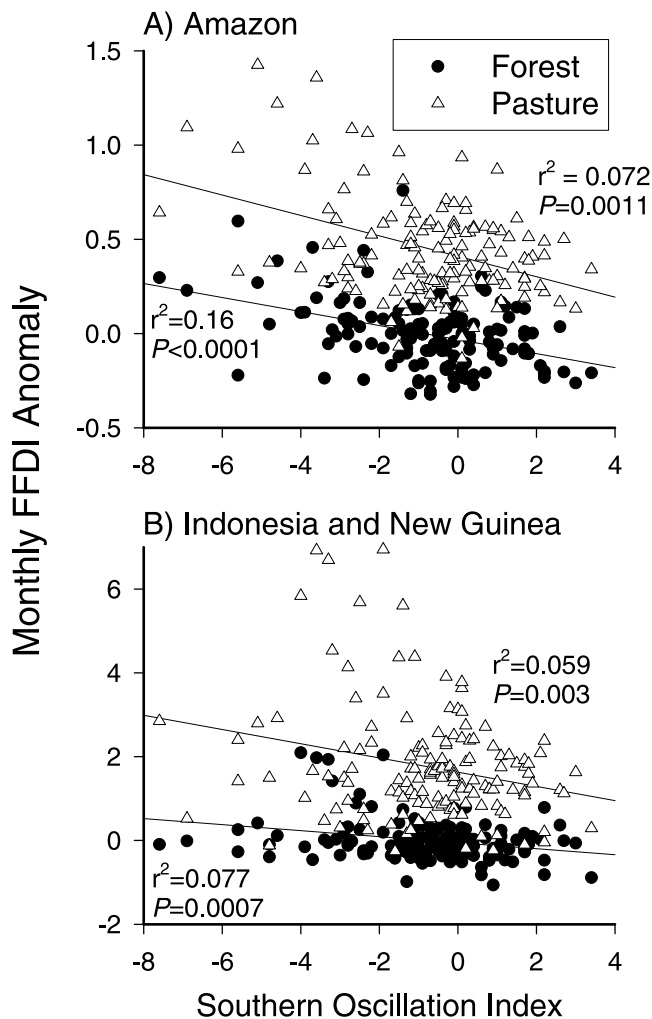
Figure 8. Relationship between Southern Oscillation Index (SOI) and relative monthly anomaly in FFDI in the Amazon Basin. The relative monthly anomaly was calculated as $(X - \overline{X}_{forest})/(\overline{X}_{forest})$ where X is the monthly mean and $\overline{X}_{forest}$ is the multiyear mean for that month under the forest scenario. Fire risk was greater under El Niño conditions (negative SOI values).

These are the areas with the lowest initial fire risks, so despite large relative increases, the contribution to regional means is relatively low. For example, in the Amazon where much of the area is predicted to experience an increase in fire number of >400% (Figure 5), the basin-wide total is expected to increase only 44%. Most fires occur in the seasonally dry forest regions near edges of the core forest areas, where there was little or no increase in fire risk following deforestation. And in the areas peripheral to the tropical forests, fire risk was reduced. However, these areas dominated by savanna vegetation are being cleared even more quickly than in the tropical forests, causing increased fire risk likely to offset the reductions seen here [*Hoffmann et al.*, 2002].

[32] Predicting future fire frequencies will require a more complete understanding of the contributions of other determinants such as greenhouse warming and ENSO. Climate change due to the greenhouse effect is likely to be additive to that caused by deforestation [*Costa and Foley*, 2000; *Zhang et al.*, 2001], so the increase in fire risk shown here will be compounded with that expected from greenhouse warming [e.g., *Flannigan et al.*, 2000; *Williams et al.*, 2001]. Furthermore, increase in fuel accumulation due to elevated CO_2 may increase fire frequency and intensity [*Sage*, 1996]. The role of El Niño is also important, since the Amazon and Indonesia experience drought during El Niño events [*Trenberth et al.*, 1998], resulting in increased fire occurrence [*Nepstad et al.*, 2001; *Siegert et al.*, 2001]. In the present study, fire risk was significantly, albeit weakly, correlated to the Southern Oscillation Index, as expected, since CCM3 generates weather patterns similar to El Niño in response to sea surface temperatures [*Meehl and Arblaster*, 1998].

[33] Several factors limit our ability to predict the effect of climate change on future fire regimes. The coarse scale of GCM is not adequate for simulating mesoscale circulations that may arise from the landscape heterogeneity resulting from tropical deforestation [*Baidya Roy and Avissar*, 2002; *Weaver et al.*, 2002]. Because of convection generated over pasture sites, mesoscale models suggest that low levels of deforestation may actually increase precipitation [*Avissar et al.*, 2002]. Also, because of the poor temporal and spatial resolution of AVHRR hot spots, the number of hot spots is not a perfect surrogate for total area burned. Furthermore, fire intensity and fuel consumption, two aspects of fires that have important consequences for forest regeneration and carbon storage, also respond to climate but cannot be resolved with the data presented here.

[34] The role of humans as the primary ignition source in tropical forest regions also introduces considerable uncertainty in how fire regimes will respond to future climates. The use of fire by humans is largely a function of socio-economic factors such as land use, population density, and distance from roads. These pressures are likely to increase ignition events in the future [*Cardoso et al.*, 2003], but here we disregard such changes to separate them from climatic impacts.

[35] Although humans set most of the fires in tropical forest regions, we can expect climate to be the primary driver of interannual variations in fire occurrence, as has been shown in other regions where fires are primarily anthropogenic [*Veblen et al.*, 1999; *Millán et al.*, 1998; *Barbosa et al.*, 1999]. Even so, possible interactions between climate and human behavior may confound estimates of climate impacts on fire occurrence. The observed relationship between FFDI and hot spot number might be partially determined by human behavior, since land owners typically burn recently deforested lands at the end of the dry season when fuel and atmospheric conditions ensure more complete combustion of the fuel. If such burning of slash accounts for all of the area burned, then climate change may not strongly increase fire occurrence, since the rate of deforestation would limit annual area burned. However, *Cardoso et al.* [2003] found that, of five variables examined, rate of deforestation was the least useful for explaining the number of observed hot spots in the Amazon. Similarly, in a study involving >900,000 ha in 202 land holdings in five regions in the Brazilian Amazon, *Nepstad et al.* [1999] found that deforestation fires accounted for only 13% of burned area, suggesting that the timing of these fires can

account for little of the correlation between FFDI and hot spot number.

[36] While human behavior may influence the relationship between FFDI and area burned by determining the timing of ignitions, it is important to note that total area burned also depends strongly on the mean area burned per ignition. The success of ignition, the rate of spread, the likelihood of escaping control, and consequently, area burned per ignition are largely determined by atmospheric conditions and fuel dryness. The FFDI takes current weather and fuel dryness into account, explaining the strong relationship between FFDI and observed fire number. These factors are likely to be particularly important for determining the number and extent of accidental burnings. In the aforementioned study, *Nepstad et al.* [1999] found that 67% of the burned area was unintentional. Climate change is likely to have a particularly strong impact on these unintentional burns by increasing the number of fires that escape control and the subsequent area burned.

6. Conclusion

[37] Climate has a strong impact on fire frequency and intensity, which in turn have strong impacts on vegetation dynamics. Consequently, fire is likely to play an important role in vegetation-climate feedbacks. This is particularly true in tropical forests, where a combination of rapid deforestation, widespread fire use, and fire-sensitive vegetation create conditions that permit such a feedback to occur.

References

Avissar, R., P. L. Silva Dias, M. A. F. Silva Dias, and C. A. Nobre, The Large-Scale Biosphere-Atmosphere Experiment in Amazonia (LBA): Insights and future research needs, *J. Geophys. Res.*, 107(D20), 8086, doi:10.1029/2002JD002704, 2002.

Baidya Roy, S., and R. Avissar, Impact of land use/land cover change on regional hydrometeorology in Amazonia, *J. Geophy. Res.*, 107(D20), 8037, doi:10.1029/2000JD000266, 2002.

Barbosa, P. M., D. Stroppiana, and J.-M. Grégoire, An assessment of vegetation fire in Africa (1981–1991), Burned areas, burned biomass and atmospheric emissions, *Global Biogeochem. Cycles*, 13(4), 933–950, 1999.

Bonan, G. B., *A Land Surface Model (LSM version 1. 0) for Ecological, Hydrological, and Atmospheric Studies: Technical Description and User's Guide*, 150 pp., Natl. Cent. for Atmos. Res., Boulder, Colo., 1996.

Bonan, G. B., The land surface climatology of the NCAR land surface model coupled to the NCAR community climate model, *J. Clim.*, 11(6), 1307–1326, 1998.

Cardoso, M. F., G. C. Hurtt, B. I. Moore, C. A. Nobre, and E. M. Prins, Projecting future fire activity in Amazonia, *Global Change Biol.*, 9, 656–669, 2003.

Cochrane, M. A., and M. D. Schulze, Fire as a recurrent event in tropical forests of the eastern Amazon: Effects on forest structure, biomass, and species composition, *Biotropica*, 31(1), 2–16, 1999.

Cochrane, M. A., A. Alencar, M. D. Schulze, C. M. Souza, D. C. Nepstad, P. Lefebvre, and E. A. Davidson, Positive feedbacks in the fire dynamic of closed canopy tropical forests, *Science*, 284(5421), 1832–1835, 1999.

Costa, M. H., and J. A. Foley, Combined effects of deforestation and doubled atmospheric CO_2 concentrations on the climate of Amazonia, *J. Clim.*, 13, 18–34, 2000.

Davies-Colley, R. J., G. W. Payne, and M. van Elswijk, Microforest gradients across a forest edge, *N. Z. J. Ecol.*, 24(2), 111–121, 2000.

Dickinson, R. E., and P. Kennedy, Impacts on regional climate of Amazon deforestation, *Geophys. Res. Lett.*, 19(19), 1947–1950, 1992.

Eltahir, E. A. B., and R. L. Bras, On the response of the tropical atmosphere to large-scale deforestation, *Q. J. R. Meteorol. Soc.*, 119, 779–793, 1993.

Flannigan, M. D., B. J. Stocks, and B. M. Wotton, Climate change and forest fires, *Sci. Total Environ.*, 262, 221–229, 2000.

Garratt, J. R., *The Atmospheric Boundary Layer*, 316 pp., Cambridge Univ. Press, New York, 1992.

Giambelluca, T. W., A. D. Ziegler, M. A. Nullet, D. M. Truong, and L. T. Tran, Transpiration in a small tropical forest patch, *Agric. For. Meteorol.*, 117, 1–22, 2003.

Hahmann, A. N., and R. E. Dickinson, RCCM2-BATS Model over tropical South America: Applications to tropical deforestation, *J. Clim.*, 10, 1944–1964, 1997.

Henderson-Sellers, A., R. E. Dickinson, T. B. Durbidge, P. J. Kennedy, K. McGuffie, and A. J. Pitman, Tropical deforestation: Modeling local-to regional-scale climate change, *J. Geophys. Res.*, 98(D4), 7289–7315, 1993.

Hoffmann, W. A., and R. B. Jackson, Vegetation-climate feedbacks in the conversion of tropical savanna to grassland, *J. Clim.*, 13, 1593–1602, 2000.

Hoffmann, W. A., W. Schroeder, and R. B. Jackson, Positive feedbacks of fire, climate, and vegetation and the conversion of tropical savanna, *Geophys. Res. Lett.*, 29(22), 2052, doi:10.1029/2002GL015424, 2002.

Holdsworth, A. R., and C. Uhl, Fire in Amazonian selectively logged rain forest and the potential for fire reduction, *Ecol. Appl.*, 7(2), 713–725, 1997.

Jackson, R. B., H. A. Mooney, and E.-D. Schulze, A global budget for fine root biomass, surface area, and nutrient contents, *Proc. Natl. Acad. Sci.*, 94, 7362–7366, 1997.

Jackson, R. B., et al., Belowground consequences of vegetation change and their treatment in models, *Ecol. Appl.*, 10, 470–483, 2000.

Keetch, J., and G. Byram, A drought index for forest fire control, 32 pp., U.S. Dep. of Agric. For. Serv., Southeast. For. Exp. Stn., Asheville, N. C., 1968.

Kiehl, J. T., J. J. Hack, G. B. Bonan, B. A. Boville, D. L. Williamson, and P. J. Rasch, The National Center for Atmospheric Research community climate model: CCM3, *J. Clim.*, 11(6), 1131–1149, 1998.

Laurance, W. F., and G. B. Williamson, Positive feedbacks among forest fragmentation, drought, and climate change in the Amazon, *Conserv. Biol.*, 15(6), 1529–1535, 2001.

Meehl, G. A., and J. A. Arblaster, The Asian-Australian monsoon and El Niño Southern Oscillation in the NCAR Climate System Model, *J. Clim.*, 11(6), 1356–1385, 1998.

Millán, M. M., M. J. Estrela, and C. Badenas, Meteorological processes relevant to forest fire dynamics on the Spanish Mediterranean coast, *J. Appl. Meteorol.*, 37, 83–100, 1998.

Nepstad, D. C., A. G. Moreira, and A. A. Alencar, Flames in the rain forest: Origins, impacts and alternatives to Amazonian fire, 161 pp., Pilot Program to Conserve the Brazilian Rain Forest, Brasilia, Brazil, 1999.

Nepstad, D., G. Carvalho, A. C. Barros, A. Alencar, J. P. Capobianco, J. Bishop, P. Moutinho, P. Lefebvre, U. L. Silva Jr., and E. Prins, Road paving, fire regime feedbacks, and the future of Amazon forests, *For. Ecol. Manage.*, 154, 395–407, 2001.

Newmark, W. D., Tanzanian forest edge microclimatic gradients: Dynamic patterns, *Biotropica*, 33(1), 2–11, 2001.

Noble, I. R., G. A. V. Bary, and A. M. Gill, McArthur's fire-danger meters expressed as equations, *Aust. J. Ecol.*, 5, 201–203, 1980.

Nobre, C. A., P. J. Sellers, and J. Shukla, Amazonian deforestation and regional climate change, *J. Clim.*, 4, 957–988, 1991.

Polcher, J., and K. Laval, The impact of African and Amazonian deforestation on tropical climate, *J. Hydrol.*, 155, 389–405, 1994.

Sage, R. F., Modification of fire disturbance by elevated CO_2, in *Carbon Dioxide, Populations, and Communities*, edited by C. Körner and F. A. Bazzaz, pp. 231–249, Academic, San Diego, Calif., 1996.

Salati, E., and C. A. Nobre, Possible climatic impacts of tropical deforestation, *Clim. Change*, 19, 117–196, 1991.

Siegert, F., G. Ruecker, A. Hinrichs, and A. A. Hoffmann, Increased damage from fires in logged forests during droughts caused by El Nino, *Nature*, 414, 437–440, 2001.

Sud, Y. C., R. Yang, and G. K. Walker, Impact of in situ deforestation in Amazonia on the regional climate: General circulation model simulation study, *J. Geophys. Res.*, 101(D3), 7095–7109, 1996.

Trenberth, K. E., Signal versus noise in the Southern Oscillation, *Mon. Weather Rev.*, 112, 326–332, 1984.

Trenberth, K. E., G. W. Branstator, D. Karoly, A. Kumar, N. C. Lau, and C. Ropelewski, Progress during TOGA in understanding and modeling global teleconnections associated with tropical sea surface temperatures, *J. Geophys. Res.*, 103(C7), 14,291–14,324, 1998.

Uhl, C., and J. B. Kauffman, Deforestation, fire susceptibility and potential tree responses to fire in the eastern Amazon, *Ecology*, 71(2), 437–449, 1990.

Veblen, T. T., T. Kitzberger, R. Villalba, and J. Donnegan, Fire history in northern Patagonia: The roles of humans and climatic variation, *Ecol. Monogr.*, 69(1), 47–67, 1999.

Weaver, C. P., S. Baidya Roy, and R. Avissar, Sensitivity of simulated mesoscale atmospheric circulations resulting from landscape heterogeneity to aspects of model configuration, *J. Geophys. Res.*, 107(D20), 8041, doi:10.1029/2001JD000376, 2002.

Williams, A. A. J., D. Karoly, and N. Tapper, The sensitivity of Australian fire danger to climate change, *Clim. Change*, 49(1–2), 171–191, 2001.

Zeng, N., R. E. Dickinson, and X. Zeng, Climatic impact of Amazon deforestation— A mechanistic model study, *J. Clim.*, 9, 859–883, 1996.

Zhang, H., A. Henderson-Sellers, and K. McGuffie, Impacts of tropical deforestation. part I: Process analysis of local climatic change, *J. Clim.*, 9, 1497–1517, 1996.

Zhang, H., A. Henderson-Sellers, and K. McGuffie, The compounding effects of tropical deforestation and greenhouse warming on climate, *Clim. Change*, 49, 309–338, 2001.

Zwiers, F. W., and H. von Storch, Taking serial correlation into account in tests of the mean, *J. Clim.*, 8, 336–351, 1995.

W. A. Hoffmann, Department of Botany, North Carolina State University, Campus Box 7612, Raleigh, NC 27695-7612, USA. (hoffmann@unb.br)

R. B. Jackson, Department of Biology and Nicholas School of the Environment and Earth Sciences, Box 90340, Phytotron Building, Duke University, Durham, NC 27708, USA. (jackson@duke.edu)

W. Schroeder, Instituto Brasileiro do Meio Ambiente e dos Recursos Naturais Renováveis, SAIN Av. L4 Norte - Bloco C – PROARCO, Brasília DF 70818-900, Brazil. (swilfrid@sede.ibama.gov.br)